

# Bose-Fermi solid and its quantum melting in an one-dimensional optical lattice

Bin Wang<sup>1</sup>, Daw-Wei Wang<sup>2</sup>, and S. Das Sarma<sup>1</sup>

<sup>1</sup>*Condensed Matter Theory Center, Department of Physics,  
University of Maryland, College Park, Maryland 20742, USA*

<sup>2</sup>*Physics Department and NCTS, National Tsing-Hua University, Hsinchu 30013, Taiwan*

We investigate the quantum phase diagram of Bose-Fermi mixtures of ultracold dipolar particles trapped in one-dimensional optical lattices in the thermodynamic limit. With the presence of nearest-neighbor (N.N.) interactions, a long-ranged ordered crystalline phase (Bose-Fermi solid) is found stabilized between a Mott insulator of bosons and a band-insulator of fermions in the limit of weak inter-site tunneling ( $J$ ). When  $J$  is increased, such a Bose-Fermi solid can be quantum melted into a Bose-Fermi liquid through either a two-stage or a three-stage transition, depending on whether the crystalline order is dominated by the N.N. interaction between fermions or bosons. These properties can be understood as quantum competition between a pseudo-spin frustration and a pseudo-spin-charge separation, qualitatively different from the classical picture of solid-liquid phase transition.

PACS numbers:

The successful experimental preparation of ultracold dipolar atoms[1] and polar molecules[2] has opened a new direction of strongly correlated physics. The long-ranged anisotropic feature of the dipolar interaction can lead to qualitatively different physics as compared to the conventional ultracold atom systems. Recent theoretical efforts have been mostly devoted to either bosonic or fermionic dipolar gases [3–5]. However, not much work is reported on dipolar Bose-Fermi mixtures, although their counterparts in conventional ultracold atoms have been extensively studied both experimentally [6] and theoretically [7–10]. When the dipolar interaction is included, some crystalline order may be realized [4], providing completely new insight onto the solid-liquid phase transition, which is one of the most important subjects in classical physics. We show in this work that a Bose-Fermi dipolar mixture allows for extremely rich interaction physics by manifesting a complex and experimentally accessible quantum phase diagram containing many exotic quantum phases hitherto not considered in cold atomic gases.

In this paper, we study various kinds of Bose-Fermi mixtures of dipolar particles loaded in an one dimensional (1D) optical lattice. Keeping only the on-site and the nearest-neighbor (N.N.) interactions, five distinct quantum phases can be identified: Bose-Fermi solid (BFS), density wave Bose-Fermi Mott state (DW-BFM), density wave Bose-Fermi liquid (DW-BFL), uniform Bose-Fermi Mott state (UBFM), and uniform Bose-Fermi liquid (UBFL), as shown in Fig. 1. The BFS phase has alternating boson and fermion densities similar to its classical counterpart, but can be quantum melted even at  $J = 0$  through an Ising-type frustration when the dipole moments of bosons and fermions are equal. When  $J$  increases, the BFS state can have another quantum melting through a multi-stage transition, which can be understood as Kosterlist-Thouless type with the pseudo-spin-charge separation[11]. We also discuss the experimental

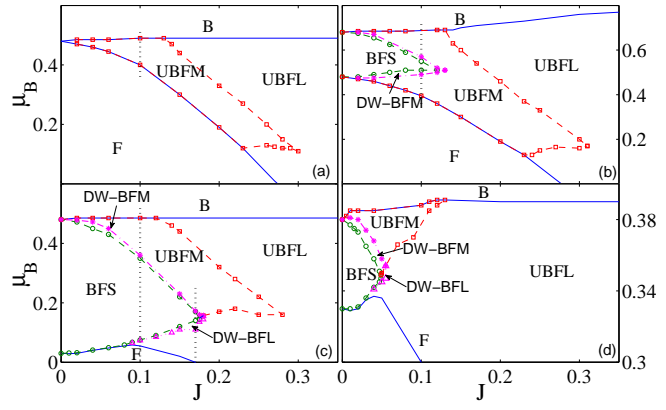


FIG. 1: Phase diagrams of dipolar Bose-Fermi mixtures: (a)-(d) corresponds to Case I-IV as defined in the text.  $V_{BB} = 0.1$  in (b) and (d), and  $V_{FF} = 0.225$  in (c) and (d).  $V_{BF} = 0.15$  in (d) and  $\mu_F = 0.48$  for all panels.  $U = 1$  is the energy unit. The vertical dotted lines in (a)-(c) show the intersect for which the particle density is presented in Fig. 3.

preparation and observation of these quantum phases, and connect our results to the metallic electronic reconstruction at the interface of a band insulator and a Mott insulator [12].

To describe our model system, we adopt the following extended Bose-Fermi Hubbard Hamiltonian:  $H = H_B + H_F + H_{BF}$ , where

$$\begin{aligned} H_B &= -J_B \sum_{\langle i,j \rangle} b_i^\dagger b_j + \frac{U_{BB}}{2} \sum_i n_i^B (n_i^B - 1) \\ &\quad + \frac{V_{BB}}{2} \sum_{\langle i,j \rangle} n_i^B n_j^B - \mu_B \sum_i n_i^B, \\ H_F &= -J_F \sum_{\langle i,j \rangle} f_i^\dagger f_j + \frac{V_{FF}}{2} \sum_{\langle i,j \rangle} n_i^F n_j^F - \mu_F \sum_i n_i^F, \end{aligned}$$

$$H_{BF} = U_{BF} \sum_i n_i^B n_i^F + V_{BF} \sum_{\langle i,j \rangle} n_i^B n_j^F. \quad (1)$$

Here,  $b_i$  and  $f_i$  are the bosonic and fermionic field operators at the  $i$ th site.  $n_i^B = b_i^\dagger b_i$  and  $n_i^F = f_i^\dagger f_i$  are density operators.  $J_a$  and  $\mu_a$  are respectively the hopping rates between adjacent sites ( $\langle i, j \rangle$ ) and chemical potentials;  $U_{ab}$  and  $V_{ab}$  describe the on-site and the N.N. interactions respectively, with  $a$  and  $b$  denoting bosons ( $B$ ) or fermions ( $F$ ). Such a system can in principle be engineered in ultracold dipolar gases. Longer range interactions are neglected here because they do not qualitatively change the phase diagram near half filling [14].

In the hard-core boson limit ( $U_{BB} \rightarrow \infty$ ) one can map the bosonic operators to fermionic ones, and the whole system can be transformed to a special extended Hubbard model with spin-dependent N.N. interactions. Such a system breaks the SU(2) symmetry and cannot be solved analytically. Since we are interested here in the interplay of quantum statistics with N.N. interactions, we will consider a soft-core case by setting  $J_a = J$  and  $U_{ab} \equiv U = 1$  for simplicity. Near the Mott insulator regime, we can reduce the Hilbert space into 0, 1 and 2 particles per site and hence such soft-core bosons can also be mapped to a spin-1 chain [5], i.e. Eq. (1) can be mapped onto a unique spin ladder composed of a spin-one chain and a spin-half chain with frustrated anti-ferromagnetic coupling as  $V_{ab} > 0$ . In our calculation, we stick with the particle model and the ground states are obtained using an infinite lattice version of the time-evolving-block-decimation (TEBD) algorithm [13], which exploits a tensor product representation of many-body states and is especially efficient for the gapped solid phase that we are interested in here.

In order to clarify the effects of the N.N. interactions, we calculate and compare the following six representative cases: Case I: neither bosons or fermions are dipolar particles, i.e.  $V_{ab} = 0$ ; Case II: only bosons are dipolar particles, i.e.  $V_{BB} > 0$  and  $V_{BF} = V_{FF} = 0$ ; Case III: only fermions are dipolar particles, i.e.  $V_{FF} > 0$  and  $V_{BB} = V_{BF} = 0$ ; Case IV: both bosons and fermions are dipolar particles, i.e.  $V_{BB}/V_{BF} = V_{BF}/V_{FF} \equiv \chi$  and  $\chi = 2/3 < 1$ ; Case V: same as Case IV but for  $\chi = 3/2 > 1$ ; Case VI: same as Case IV but for  $\chi = 1$ . Several representative quantum phase diagrams are shown in Fig. 1, where panels (a)-(d) correspond to Case I-IV respectively. Results of Case V and Case VI are qualitatively the same as Case II and Case I respectively. To save space, we do not show their phase diagrams here.

In the limit of small(large)  $\mu_B$ , the system is a pure Fermi(Bose) gas, denoted by  $F(B)$ . Within these parameters, the ground state can be a bosonic Mott insulator or a 1D Bose liquid in regime B, while in regime F it can be a band insulator or a Fermi liquid. In the mixed regime, there are five distinct quantum phases to be ob-

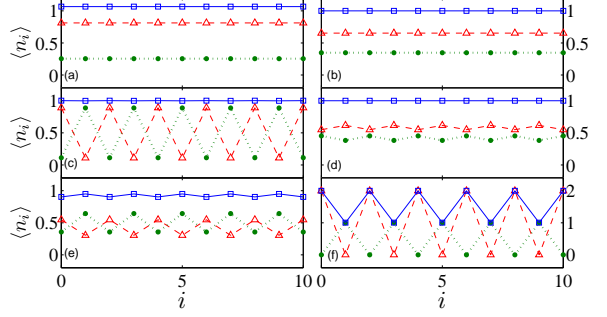


FIG. 2: Typical real space distributions of boson (open triangle), fermion (filled circle), and total density (open diamond) in (a) UBFL, (b) UBFM, (c) BFS, (d) DW-BFM, and (e) DW-BFL phases. Panel (f) shows a BFS phase with higher filling fraction of bosons.

served: (i) in the large  $J$  regime, we have a UBFL phase, whose quasi-long-ranged order can be obtained by using bosonization[8]. The density distribution is uniform in space for each species, as shown in Fig. 2(a). (ii) In the regime of stronger interaction, there is a UBFM phase, where the total filling fraction is found to be unity through the entire regime with a gapped excitation. The UBFM phase exists even without N.N. interaction (Fig. 1(a)) [10], and it has a uniform and compressible inter-species density difference (Fig. 2(b)). (iii) When the N.N. tunneling is close to zero, we find a BFS phase, where both species are at half-filling but have an alternating density pattern (see Fig. 2(c)). Such a phase is incompressible for both species (i.e.  $\partial \langle n_i^a \rangle / \partial \mu_b = 0$  for  $a, b = \{B, F\}$ ), while their density oscillation amplitudes decrease as  $J$  increases. (iv) Near the boundary between BFS and UBFM, there is a narrow regime, where the BFM phase has a density wave order (DW-BFM), i.e.  $\langle n_i^B - n_i^F \rangle$  oscillates periodically while the total filling remains integer (see Fig. 2(d)). (v) Finally, near the boundary between BFS and BFL, we find a BFL with a density wave order in both species (named DW-BFL). Different from DW-BFM, DW-BFL is compressible with an incommensurate total filling fraction (Fig. 2(e)). This phase can also be regarded as a supersolid phase in the quasi-long-ranged order sense.

In Fig. 2(a)-(e), we show typical spatial density distributions for BFL, UBFM, BFS, DW-BFM, and DW-BFL phases respectively. We note that, although the true spin-charge separation exists only in the low energy regime [8], we can still phenomenologically define the pseudo-charge to be  $\langle n_i^B + n_i^F \rangle$ , and pseudo-spin to be  $\langle n_i^B - n_i^F \rangle$ . As a result, the BFL phase has gapless excitations in both pseudo-charge and pseudo-spin sectors, UBFM has a gapped charge excitation, and BFS has gapped excitation in both sectors. DW-BFM has a gapped pseudo-charge excitation with a gapless pseudo-spin-density wave order, while DW-BFL has two gapless

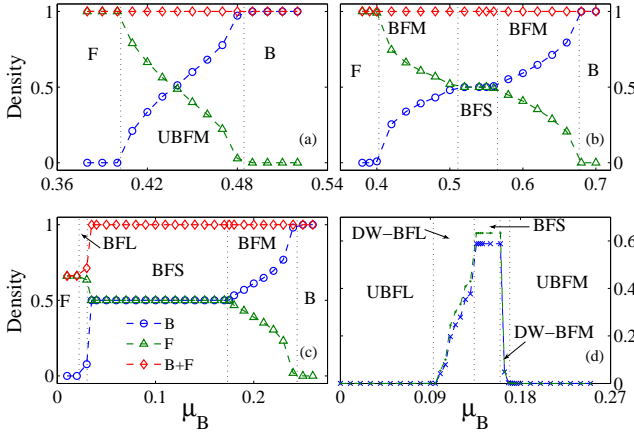


FIG. 3: (a)-(c) Average boson (circle), fermion (triangle), and total (diamond) densities as functions of  $\mu_B$  at  $J = 0.1$ . All other parameters are the same as in Fig. 1(a)-(c) respectively. (d) shows the density wave order at  $J = 0.17$  for the same system as in (c). The solid dot and check markers correspond to the density wave order,  $|\langle n_i^B \rangle - \langle n_{i+1}^B \rangle|$  and  $|\langle n_i^F \rangle - \langle n_{i+1}^F \rangle|$ .

excitations on top of the pseudo-spin density wave order. Note that our numerical calculation is for an infinite 1D system, so the observed density wave order is always a truly long-ranged order. In Fig. 3(a)-(c), we further plot the average filling fraction of bosons and fermions (together with the total fraction) as a function of the bosonic chemical potential  $\mu_B$ , showing the regime of different phases. The plateau for particle density at 0.5 in panels (b) and (c) corresponds to the half-filled BFS phase. The plateau of total density at unity can be identified to be a Mott phase if densities of individual species vary as a function of the chemical potential. Finally, the regime with a varying total density corresponds to the BFL phase. UBFM and DW-BFM cannot be distinguished here (same as UBFL and DW-BFL) since only the average filling fraction is shown. In Fig. 3(d), the density wave order is plotted as a function of  $\mu_B$  at  $J = 0.17U$ , and is found to disappear continuously when changing  $\mu_B$  away from BFS regime.

Note that the origin of our BFS state is different from that of the Neel(Ising) state predicted in [9], where no N.N. interaction exists. In the latter case, the effective long-ranged interaction between heavier species is induced by the quantum fluctuations of the lighter species, and becomes effectively vanishing when  $J_B = J_F$ . Besides, we also note that at higher  $\mu_B$  (outside the regime of Fig. 1), a BFS state with more than one particle per site is also possible (see Fig. 2(f)), but we will not discuss such phases here due to space limitation.

To gain more insight on the crystalline phase, it is instructive to look into the classical limit at  $J = 0$ , where no difference between fermionic and bosonic particles is expected. By comparing the energies of various configurations, for example, half-filled Bose/Fermi density

wave, Bose Mott Insulator, and half-filled BFS, we can obtain the necessary condition for a BFS phase to be:  $\mu_B, \mu_F > 2V_{BF}$  and

$$2(V_{FF} - V_{BF}) > \mu_F - \mu_B > 2(V_{BF} - V_{BB}). \quad (2)$$

It is therefore interesting to find that for a symmetric case, i.e. Case VI and  $V_{ab} = V$ , a crystal exists only when  $\mu_F = \mu_B > 2V$ , and the state  $\{\cdots BFBF\cdots\}$  would be degenerate with all states of one particle per site. This can also be understood in the spin-ladder picture we described earlier: the N.N. interactions,  $V_{ab} > 0$ , provide an Ising-type frustration, namely,  $V_{BF}$  competes with  $V_{BB}$  and  $V_{FF}$ , and hence smear out the anti-ferromagnetic order. At a finite but small  $J$ , the degeneracy is removed, but the density wave order is still so small that the BFS phase just disappears when  $\mu_B$  slightly differs from  $\mu_F$ . Therefore, according to our numerical calculation and conditions in Eq. (2), we conclude that the BFS phase is unlikely to be observed in a realistic experimental situation for the symmetric case ( $\chi = 1$ ) due to the frustrated nature of the dipolar mixture. The system is therefore still compressible and uniform in density, as the UBFM case shown in Fig. 1(a).

Away from the symmetric case, we first consider the pro-boson case, i.e. the N.N. interaction between bosons is stronger than that between fermions ( $\chi > 1$ ) and hence dominates the crystal order formation. For such a situation, we show our results for Case II in Fig. 1(b). Results for Case V are similar. Such pro-boson BFS is quantum melted to the UBFL via a three-stage process: first, the ground state has a second order transition toward the DW-BFM phase, having a compressible pseudo-spin density wave order on top of a pseudo-charge Mott phase. When  $J$  becomes slightly larger, the density wave order disappears and the ground state becomes a UBFM phase, where the single particle Green's function decays exponentially (see Fig. 4). Finally, the pseudo-charge gap of UBFM becomes zero at larger  $J$ , leading to a BFL phase. The last two transitions should belong to the Kosterlitz-Thouless universality class in the pseudo-spin and pseudo-charge sectors respectively, as described by an X-Y model in the 1+1 dimensional system.

However, such kind of three-stage process from BFS to BFL does not always exist for a pro-fermion case, i.e. when the crystal order is mainly provided by the N.N. interaction between fermions. We provide the quantum phase diagrams for both Case III and Case IV in Figs. 1(c) and (d). In Fig. 1(c), we find that in addition to the three-stage melting process discussed above, in the lower portion of the BFS boundary, there is a different melting process: first from BFS to DW-BFL and then from DW-BFL to UBFL.

Such different melting processes for pro-boson and pro-fermion solids demonstrate the quantum character of BFS. Their common feature is the smooth decrease of the density wave order when outside the BFS phase, while

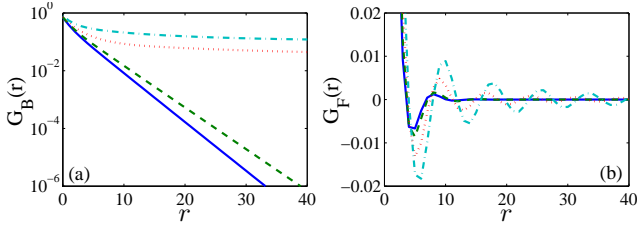


FIG. 4: Green functions for (a) bosons and (b) fermions in a few samples inside the UBFM and UBFL phase.  $J = 0.15, 0.16, 0.17, \text{ and } 0.18$  for the solid, dashed, dotted, and dash-dotted lines respectively.  $\mu_B = 0.4$  and all other parameters are the same as in Fig. 1(c).

the difference lies in that the pseudo-charge gap disappears together with the pseudo-spin gap in the lower portion of BFS boundary for the pro-fermion case. This result can be understood when comparing the BFS regime in Fig. 1(b) and (c). First, without N.N. interaction (Fig. 1(a)), the BFS is degenerate with other states at a single point,  $\mu_B = \mu_F$  and  $J = 0$ . When  $V_{BB} > 0$  and other  $V_{ab} = 0$ , from the condition shown in Eq. (2), the regime of BFS is  $0 < \mu_B - \mu_F < 2V_{BB}$ , i.e. the BFS regime is entirely inside the original Mott insulator regime. As a result, when BFS is melted, the whole system is still in the regime of commensurate total filling fraction, and a Mott phase with a pseudo-charge gap is then expected in the strong interaction limit. On the other hand, when only  $V_{FF} > 0$  and other  $V_{ab} = 0$ , the condition for BFS at  $J = 0$  gives  $0 < \mu_F - \mu_B < 2V_{FF}$ , which is inside the regime of fermion band insulator as shown in Fig. 1(a). Unlike Mott insulator for bosonic particles, the band insulator of fermions exists in non-interacting limit and hence can be easily destroyed by finite interactions, leading to a Luttinger liquid in 1D with incommensurate filling. That is why both pseudo-spin and pseudo-charge gaps disappear in the DW-BFL and UBFL regimes when BFS is melted in the lower boundary of BFS phase in Fig. 1(c). The nature of such a transition is still unclear. Finally, from Fig. 1(d), we can see that the phase diagram for such a pro-fermion case is qualitatively similar to Fig. 1(c), but the finite value of  $V_{BF}$  can suppress the BFS phase as well as the BFM phase, consistent with the fact that no BFS exists in the symmetric case due to Ising-type frustration.

In Fig. 4 we also present the single particle Green's function of (a) bosons:  $G_B(r) = \langle b_i^\dagger b_{i+r} \rangle$  and (b) the fermions,  $G_F(r) = \langle f_i^\dagger f_{i+r} \rangle$ . It clearly shows that the single particle correlation of bosons and fermions has an exponential decay in the UBFM regime (solid and dashed lines), while they have a slower algebraic decay due to the quasi-long-ranged order inside the UBFL regime (dotted and dashed-dotted lines).

Before concluding, we note that the system we discuss here can be easily realized by a mixture of dipolar

atoms/molecules loaded into a 1D optical lattice. One may provide two separate trapping potentials for bosons and fermions, and prepare them to be a Mott insulator and a band insulator respectively. When the relative distance between these two traps is getting smaller, the intermediate regime between these two clouds experiences a continuous change of chemical potentials, making a potential realization of BFS and other exotic phases discussed here. Our results indicate that observing a BFS could be very challenging for systems in which bosons and fermions have close dipole moments (say  $^{39}\text{K}^{87}\text{Rb}$ - $^{40}\text{K}^{87}\text{Rb}$  or  $^{52}\text{Cr}$ - $^{53}\text{Cr}$ ), due to strong frustration. It is therefore more promising to consider a mixture of dipolar and non-dipolar particles to realize a BFS. It is interesting to note that, compared to the metallic and ferromagnetic interface of an electronic band insulator and a Mott insulator [12], the intermediate BFS phase here is an insulator with anti-ferromagnetic order, which can be easily observed in a time-of-flight measurement.

In summary, we have studied the ground-state phase diagram of the Bose-Fermi Hubbard model with arbitrary N.N. interactions. We discover the possibility and the condition to find a novel Bose-Fermi solid phase, which has a nontrivial quantum melting due to the mixture of quantum statistics even in 1D. This system can be experimentally realized within the present technique.

We acknowledge fruitful discussion with H.-H. Lin. DWW appreciates the hospitality of JQI during the initial discussion of this work. This work is supported by JQI AFOSR MURI.

- 
- [1] J. Stuhler *et al.*, Phys. Rev. Lett. **95**, 150406 (2005); for a review, see T. Lahaye, *et al.*, Rep. Prog. Phys. **72**, 126401 (2009), and reference therein.
  - [2] K.-K. Ni *et al.*, Science **322**, 231 (2008); for a recent review, see L.D. Carr and Jun Ye, New J. Phys. **11** 055009 (2009).
  - [3] M. A. Baranov, Phys. Rep. **464**, 71 (2008); Roman M. Lutchyn, Enrico Rossi, and S. Das Sarma, arXiv:0911.1378; B.M. Fregoso and E. Fradkin, Phys. Rev. Lett. **103**, 205301 (2009); D.W. Wang *et al.*, Phys. Rev. Lett. **97**, 180413 (2006); Büchler, H. P. *et al.* Phys. Rev. Lett. **98**, 060404 (2007).
  - [4] G. Pupillo, *et al.*, Phys. Rev. Lett. **100**, 050402 (2008).
  - [5] E.G. Dalla Torre, *et al.*, Phys. Rev. Lett. **97**, 260401 (2006), and reference therein.
  - [6] K. Günter, *et al.*, Phys. Rev. Lett. **96**, 180402 (2006); S. Ospelkaus *et al.*, Phys. Rev. Lett. **97**, 120403 (2006); Th. Best *et al.*, Phys. Rev. Lett. **102**, 030408 (2009).
  - [7] A. Albus, F. Illuminati, and J. Eisert, Phys. Rev. A **68**, 023606 (2003); M. Lewenstein *et al.*, Phys. Rev. Lett. **92**, 050401 (2004); D.-S. Lühmman *et al.*, Phys. Rev. Lett. **101**, 050402 (2008); I. Titvinidze, M. Snoek, and W. Hofstetter, Phys. Rev. Lett. **100**, 100401 (2008); R. M. Lutchyn, S. Tewari, and S. Das Sarma, Phys. Rev. A **79**, 011606 (2009); S. Tewari, R. M. Lutchyn, and S. Das

- Sarma, Phys. Rev. B **80**, 054511 (2009); D.-W. Wang, *et al.*, Phys. Rev. A **72**, R051604, (2005).
- [8] L. Mathey *et al.*, Phys. Rev. Lett. **93**, 120404 (2004); L. Mathey and D.-W. Wang, Phys. Rev. A **75**, 013612 (2007).
- [9] L. Pollet, M. Troyer, K. Van Houcke, and S. M. A. Rombouts, Phys. Rev. Lett. **96**, 190402 (2006).
- [10] P. Sengupta and L. P. Pryadko, Phys. Rev. B **75**, 132507 (2007).
- [11] The 2D classical melting is described by the seminal Kosterlitz-Thouless-Halperin-Nelson-Young (KTHNY) theory, which suggests a two-stage process mediated by the pairwise creation of topological defects.
- [12] S. Okamoto and A.J. Millis, Nature **428**, 630 (2004).
- [13] G. Vidal Phys. Rev. Lett. **91**, 147902 (2003); *ibid.* **93**, 040502 (2004); *ibid.* **98**, 070201 (2007).
- [14] B. Capogrosso-Sansone *et al.*, Phys. Rev. Lett. **104**, 125301 (2010).